2008 IEEE International Conference on
Robotics and Automation
Pasadena, CA, USA, May 19-23, 2008

A Robotic Needle Guide for Prostate Brachytherapy

Septimiu E. Salcudean, *Fellow, IEEE,* Thomas D. Prananta, William J. Morris and Ingrid Spadinger

***Abstract*—Low dose rate prostate brachytherapy involves the permanent implant of radioactive sources into the prostate region using needles. We present a four-degree-of-freedom robot for prostate brachytherapy. The robot can translate a needle guide in the *X*-*Y* plane allowing for precise needle insertion along the *Z* direction. It can also rotate the guide about the *X* and *Y* axes, providing thus fine control over the needle insertion point and angle. The robot is light and mountable on a standard brachytherapy stepper. It is non-back-drivable providing a stable needle insertion direction when the power is off. It allows for manual control of each of the motor axes for fine positioning and has a quick-release mechanism for gross translation of the needle guide.**

We present the robot design and the performance characteristics of the prototype we built. The robot has an interface that allows the guide to be stepped through a complete treatment plan. A radiation oncologist implanted a phantom according to a treatment plan. Only 32 minutes were required for the complete implant that had 26 needles with 136 seeds. This demonstrates that, in spite of its increased flexibility of use, the robotic guide does not add to the procedure time.

I. Introduction

BRACHYTHREAPY is a widely used treatment for prostate cancer. The treatment consists of the placement of radioactive seeds in the prostate and peri-prostatic region using trans-perineal insertion of needles, in a pattern that delivers a sufficient radiation dose to kill the cancer while maintaining a tolerable dose to the urethra and rectum [1]. Typically, B-mode ultrasound and X-ray fluoroscopy provide image guidance during prostate brachytherapy.

Reported trends indicate sharp increases in the use of brachytherapy as a treatment in patients with low-risk tumor characteristics, while the proportion of patients with low-risk tumors has also increased dramatically [2]. Based on the high detection rates in recent screening and prevention trials, there is a consensus that the number of diagnosed cases will increase sharply due to increased participation in screening. Therefore, we expect that brachytherapy use will also rise.

Manuscript received September 14, 2007. This work was supported in part by the National Science and Engineering Research Council of Canada and by the Canadian Institutes of Health Research.

S.E. Salcudean (corresponding author) (tims@ece.ubc.ca) and T.D. Prananta (tpranant@ece.ubc.ca) are with the Department of Electrical and Computer Engineering, The University of British Columbia, 2332 Main Mall, Vancouver, BC, V6T-1Z4, Canada, (604) 822-3243.

W.J. Morris (JMorris@bccancer.bc.ca) is with the Department of Radiation Oncology, and Ingrid Spadinger (ispading@bccancer.bc.ca) is with the Department of Medical Physics, both part of the Vancouver Cancer Centre, British Columbia Cancer Agency, 600 West 10th Avenue, BC, V5Z-4E6, Canada, tel. (604) (604) 877-6000.

While biochemical and clinical relapse rates are very low with current brachytherapy procedures, a number of studies report significant and wide-ranging complication rates. Complications due to brachytherapy include erectile dysfunction, urinary retention, incontinence and rectal injuries. Complications have been associated with high dose loads to large portions of the prostate [3], to high urethral dose [4] and to needle trauma [5]. A reduction in seed placement errors may lead to lower complication rates.

Poor visualization of the prostate [6], prostate movement due to needle insertion forces [7] and prostate swelling and deformation caused by edema [8] can lead to seed placement errors. Pubic arch interference with some of the parallel trajectories generated by treatment planning systems can also cause seed placement errors, because pubic arch interference requires the re-positioning of the guiding templates presently used which in turn increases inaccuracy and procedure time.

A system for more accurate delivery of needles would be beneficial for the prostate brachytherapy procedure. We summarize below some of the robotic approaches and devices developed for brachytherapy needle insertion.

Fichtinger *et al.* have proposed a system for robot-assisted prostate brachytherapy [9]. The same group has developed a 4-DOF robot assistant for guiding needles [10]. The robot is compatible with present template mounting systems.

Yu *et al.* [11] have developed a prostate brachytherapy robotic system. The system is cart-mounted and integrates a coarse motion stage, trans-rectal ultrasound probe control and a needle driver unit.

In [12], the authors evaluate robotic needle guidance using a commercial robot. The same group reported a 4-DOF robotic needle guide having a closed cylindrical closed kinematic chain with 13 linkage elements and brakes [13].

Bassan *et al.* [14] report a macro-micro approach including a 5-DOF remote center of compliance robot arm supported by a passive arm. The system features back-drivable joints with redundant sensing. The authors report targeting accuracy for a phantom implant.

Other groups have developed image-guided needle insertion systems that use fluoroscopy, CT and MRI, see, e.g. [15]. While most of the image guidance approaches presented before have only relied upon 3-D geometric models of tissue, deformation models have started to be used for needle planning, first in 2-D [16], then in 3-D [17]. Needle-tissue interaction models continue to be developed based on fluoroscopic [18] and ultrasound imaging [19].

In this paper, we present a new robotic needle guide referred to as "Brachyguide". Brachyguide is closest in concept to the system presented in [10], which employs a modified version of the robot described in [20]. Of the robotic systems surveyed above, only the robot described in [10] and Brachyguide are mounted on standard brachytherapy steppers and are compatible with the present brachytherapy procedure treatment planning systems and workflow. Brachyguide has additional features not present in any of the other systems presented to date. In particular, Brachyguide is inherently safe as it locks in position when the power is off without the need for braking mechanisms. While the needle guide itself is not backdrivable, each actuator is manually backdrivable and each degree of freedom has full manual control. The actuators are aligned with the natural degrees of freedom for needle placement and pointing. Therefore, both the user and the computer can control the needle guide location. Furthermore, the manual positioning for needle translation features a quick–release mechanism that allows fast gross positioning over the entire translation range of the device.

We present the Brachyguide design in Section II, followed by a description of its characteristics in Section III, a description of its interface and its use for a phantom implant in Section IV and a discussion in Section V. We present conclusions and plans for future work in Section VI.

II. Robot Design

We will first present an overview of the ultrasound-guided prostate brachytherapy procedure, from which we can derive a set of specifications for a robotic guide.

A. Brachytherapy Procedure and Robot Specifications

In prostate brachytherapy, small radioactive capsules or seeds are implanted in the prostate. Typically, and as done at the British Columbia Cancer Agency, a radiation oncologist images the patient's prostate during a pre-operative visit using B-mode trans-rectal ultrasound (TRUS). Transversal images (*XY* plane) acquired at regular TRUS insertion depths (*Z* axis) are segmented by hand to create a 3D model of the prostate. A Medical Physicist generates a treatment plan, using software tools, to deliver a sufficient radiation dose to kill the prostate cancer while maintaining a tolerable dose to the urethra and rectum. The plan consists of individual seed locations placed at different depths along a number of parallel lines – the planned needle insertions - passing through a rectangular *XY* plane grid (Fig. 1).

After the pre-operative visit (3-5 weeks), the patient is taken to an operating room where a Radiation Oncologist or Urologist executes the plan. The procedure is carried out under general or spinal anesthesia. To begin with, the physician manually aligns the TRUS, using US images, so that the pre-operative and intra-operative ultrasound images are registered to each other. This is done by using the coarse and fine adjustments of a brachytherapy stabilizer such as

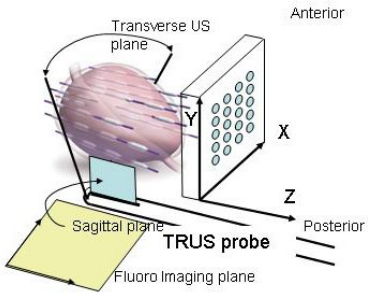

Fig. 1. Set of parallel needle insertions planned through the prostate and peri-prostatic tissue. The needles are inserted through the guidance template under TRUS guidance. Mainly the transverse plane is used to verify the needle tip location against a grid superimposed in the image.

the Micro-Touch® device (CIVCO Medical Solutions, Kalona, Iowa). The physician adjusts the TRUS depth and angle relative to the prostate by using a "stepper" unit (e.g., CIVCO EXII) mounted onto the stabilizer. An *XY*-plane insertion template attaches to the stepper. The template has a rectangular array of 13x13=169 guiding holes. The 60 mm by 60 mm template guides the needles which are inserted one by one through the perineum to the planned coordinates. A brachytherapy technician reads the coordinates in sequence. The radiation oncologist uses the guiding template, which has coordinate labels on it, to insert each needle to the planned coordinates, then pulls the needles out, leaving the seeds in the prostate. Typically, he or she inserts 80 to 130 seeds with 20 to 35 needles. Throughout the procedure, the radiation oncologist relies upon real time TRUS imaging to ensure that he/she inserts the needle tip at the planned coordinates. Fluoroscopic anterior-posterior projections are acquired to show a 2D (*ZX* plane – Fig.1) projection of the implanted seeds.

Several factors affect the accurate delivery of needles to the planned location. First, stabilizer re-positioning of the stepper is required often because needle paths often interfere with the pubic arch. Re-positioning causes registration errors. Second, tissue deformations caused by needle insertion translate and rotate the prostate causing targeting errors even if the physician placed the needle perfectly at the required geometrical spatial location. Third, tissue deformation caused by motion or edema during the procedure cause the seeds to move relative to the planning volume and therefore affect the delivered dose.

In view of the above brachytherapy procedure, a robotic guide should allow for angled needle insertions, without the minimum distance between needles imposed by the grid, over a translational workspace of at least 60 mm by 60 mm. Such a system would keep most of the legacy treatment planning systems and procedures intact. The guide should be easy to position for TRUS insertion and registration with the volume study, and, therefore, it should be light. The system should be safe and allow for quick recovery from computing system or controller errors. The angular motion range required is typically limited due to interference with the

TRUS or pubic arch. The robot should not interfere with the TRUS probe and should allow as broad a view of the operating field as possible.

B. Robot Design and Characteristics

We propose to use a very simple decoupled design. Photographs are shown in Figs. 2, 3 and 4. The robot kinematic configuration is shown schematically in Fig. 4.

A two-axis wrist is positioned by a translation stage consisting of two stacked nickel-plated aluminum dovetail linear lead-screw drives (A15 Unislide, Velmex Inc., Bloomfield, NY) with low-friction Teflon bearings. The first translation stage in the *Y* (vertical) axis is mounted to the brachytherapy stepper (CIVCO EXII). The slider of the *X*-axis Unislide is mounted to the slider of the *Y*-axis Unislide. There are no additional frames required other than the slide frames themsleves. The motion range of each of the translation axes is 150 mm. This is signficantly larger than needed, but is useful at the prototyping stage. The size can be trimmed back by cutting the Unislides to size after some experience with the device has been obtained.

The Unislide stages are driven by M6 (1mm/turn) screws actuated by 22 mm servomotors (Model 2232, Faulhaber-Group, Schonaich, Germany) aligned behind the Unislides and geared (3.125 ratio) through spur gears housed as shown in Fig. 2. The Unislide screws can also be turned manually by cranks that rotate the lead screws directly.

Mounted to the frame of the *X*-axis Unislide is the wrist. It consists of two precision rotation stages (Model 7R174-11 by Standa, Vilnius, Lithuania), mounted orthogonally to each other, as shown in Figs. 3, 4. The yaw (θ_Y) rotation stage carries the pitch (θ_X) stage. In order to avoid interference with the TRUS, normally positioned under the needle holder mounted to the wrist, a parallelogram linkage is used to move the center of rotation close (l_Y =10mm) to the needle holder. The linkage uses a Kevlar belt. The rotation stage worm gears are actuated by 17 mm servomotors (Model 1723, Faulhaber-Group). Turning dials have been attached between the wrist motors and rotation stages in order to allow manual control. The worm gear ratio is 3 degrees/turn. The parallelogram linkage limits the range of the pitch angle to $\pm 30^o$. The range of the yaw angle is limited by the interference with the translation stage but is at least $\pm 30^o$.

All motors are high speed DC coreless servomotors and are able to rapidly move the guide to planned locations. Motors were specified based on the payload and the linear and rotational friction forces measured with a number of slides and rotational stages, with a safety factor of 10 to account for the large variation in friction levels. All motors use magnetic 512 count incremental encoders. Translation sensing is redundant. Caliper-based linear inductive digital sensors were used (303-9303, Shars Tool Inc., IL). These sensors are interfaced to the computer via a synchronous serial connection, have liquid crystal displays that can be zeroed by the user and have markings in millimeter increments.

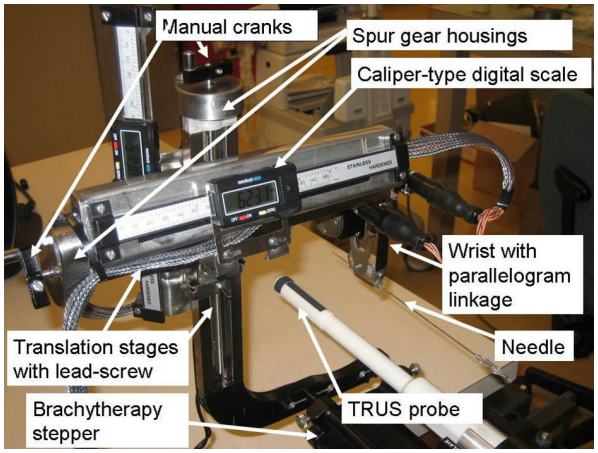

Fig. 2. Photo of the Brachyguide robot summarizing the design. The wrist details are provided in Fig. 43

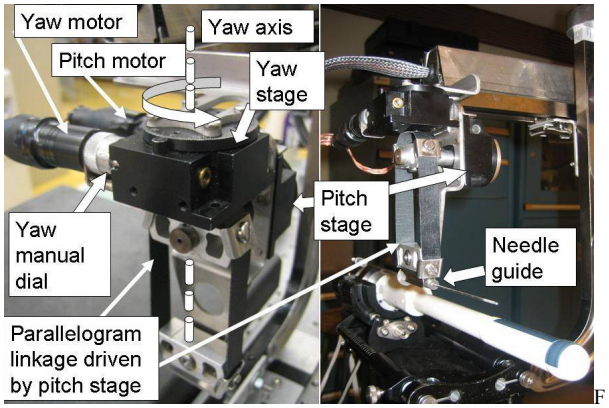

Fig. 3. Brachyguide wrist showing micrometers, wrist motors , parallelogram linkage, needle guide, needle and TRUS probe.

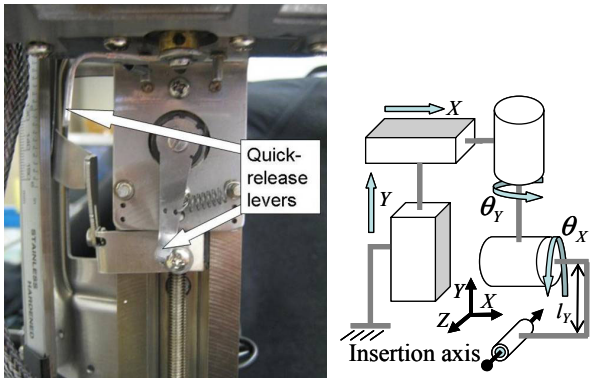

Fig. 4. Left: Quick release mechanism. When the lever is turned against the spring, the lead screw nut is disengaged.
Right: Kinematic representation of the BrachyGuide.

The wrist angles do not have redundant sensors, but the angles can be read on dials with a reading accuracy of 0.05^o. Since the rotation stages are not backdrivable, a single calibration of the angle using the ultrasound transducer and a needle can be used to re-position the needle using the motor encoder reading with the micrometer reading used as a visual check.

A cylindrical needle guide snap-mounts under the wrist pitch parallelogram linkage using a "fuse-holder" flexure.

For manual positioning in the translational axis, one turn of the crank moves the Unislide slider only one millimeter. Therefore, assuming an angled needle insertion and a worst case scenario where one needs to manually move the guide from one extreme position of the workspace to another, 150 crank turns are required! In order to avoid this and to provide another layer of safety we have designed into the slider a quick-release mechanism as shown in Fig. 4.

For the quick release mechansim, each of the nuts engaged onto the Unislide leadscrews have been milled for M6 clearance at an angle with respect to the lead screw. Thus each of the lead screw nuts can rotate through a central axis orthogonal to the leadscrew and allows one to disengage the drive when turned. The screws are turned using the levers shown. When released, the spring-loaded levers return the nuts to their normal state of being engaged to the leadscrew.

Even when making use of angled needle insertions, we do not expect that the needles will be at angles larger than 15°, as this translates into a needle tip offset of tens of millimeters. Even to traverse a 30° angle, the number of turns needed is limited to 10. Therefore, a quick release mechanism is not necessary for rotation.

Each robot axis is controlled by its own microcontroller (MCDC 3003S, Faulhaber-Group). The parameters of the motor PID controllers were set using the Faulhaber user interface provided for these controllers, which accept point-to-point moves with specified end-conditions. The individual controllers are coordinated by a motion planner from a single PC with a simple graphical user interface shown in Fig. 5.

The motion planner is simple as both the direct and inverse kinematics are straightforward from Fig. 4. We define a needle insertion point plane to be parallel to the *XY* plane and passing through the wrist yaw (*Y*) axis. We use the intersection of a desired needle insertion axis with this plane and the needle desired pitch angle θ_X to find the location of the wrist center using elementary trigonometry.

The interface allows stepping through a pre-determined set of needle guide coordinates corresponding to the planned needle insertions plan. Alternatively, the coordinates can be typed in or arrived at by an operator using an input device. In our current implementation, one of the joysticks of a USB game controller (Logitech Wingman) controls the translational velocity, while the other controls the angular velocity of the needle guide.

III. Brachyguide Characterization

Table 1 presents the Brachyguide characteristics.

We obtained the accuracy measurements by using an interferometer (ML10, Renishaw PLC, Gloucestershire, UK) to measure the errors along the horizontal and vertical axes separately. As shown in Fig. 6, encoder readings for moves

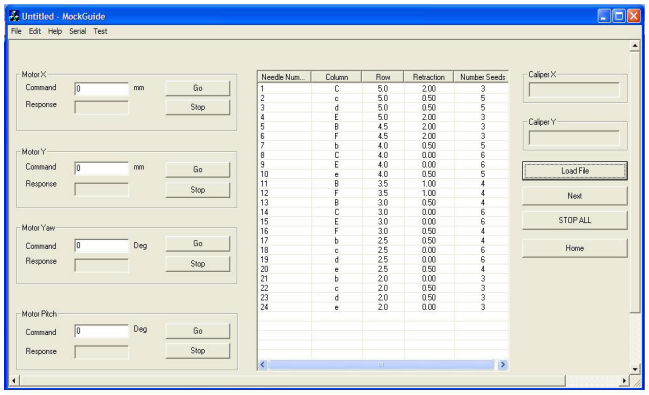

Fig. 5. Brachyguide user interface. Left side allows coordinates to be typed for each needle. Middle table shows needle number, coordinates, depth and number of seeds (four columns of six shown presently).

in a single direction fall within 0.15 mm from the interferometer readings for the full 150 mm of travel. Commanded random motions fall within 0.3 mm of the interferometer readings. As can be seen from Fig. 6, the errors are due primarily to backlash in the lead screw nuts. We plan to reduce the backlash error by pre-loading.

The digital caliper scales provide readings within 0.06 mm of the interferometer measurements. These provide the upper limit on the translation accuracy.

We measured the deviation from straight motion by mounting a digital depth gauge to the needle holder against a granite flat and commanding a full travel translation.

The rotation stage manufacturer specifies an angular accuracy of 0.05°. We verified this by using the angle measurement option of the interferometer over a range of $\pm 2^{o}$. Fig. 7 shows a typical measurement trace.

We determined the stiffness by applying a force through a load cell (MDB-2.5, Transducer techniques, Temecula, CA) to the needle guide in the *X* and *Y* axes and measuring the needle guide deflection using the interferometer.

Fig. 8 shows the robot *Y*-axis stiffness compared to the stiffness of the Civco EXII stepper mounted on the Brachystand. As can be seen, the Brachyguide frame is significantly stiffer than the mounting base, which has a stiffness of 2600 N/m in the *X*-axis and 6500 N/m in the *Y*-axis. At torque levels that keep the brachytherapy needles in their elastic region, the effect of needle torque on the Brachyguide wrist is negligible.

The point-to-point move times were determined from the encoder traces corresponding to commands for the listed motion ranges.

IV. Brachyguide Use in Phantom Study

A mock implant into a prostate phantom (model 053, CIRS Inc., Norfolk, Virginia) was performed. The setup shown in Fig. 9 was used. The Brachyguide was mounted on the EXII stepper of the CIVCO MicroTouch stabilizer.

TABLE I: BRACHYGUIDE CHARACTERISTICS

Mass		2.6 Kg
Translational workspace		150×150 mm^2
Pitch and Yaw range[1]		(-30°, 30°)
Translational accuracy[2]		<0.3 mm
Deviation from straight motion		< 0.1 mm
Rotational accuracy[2]		< 0.05° over ± 2°
Caliper accuracy	Max	0.06 mm
	Mean	0.022 mm
	Std. Dev.	0.014 mm
Point-to-point move time		
60 mm		< 2 s
150 mm		< 4.6 s
30 degree		0.7 s
Stiffness X-axis		9200 N/m
Stiffness Y-axis		15500 N/m

[1]Determined by collisions and the range of operation of the parallelogram linkage.

[2]Based on encoder values, the computed resolution is much better (0.00065 mm and 0.0058°). Maxima, not mean and standard deviation are reported, as backlash is the overwhelming cause of the error, and backlash errors have a bimodal, not a Gaussian shaped distribution. Actual resolution/accuracy are limited by backlash, flexing, etc.

An ultrasound machine (Sonix RP, Ultrasonix Medical Corporation, Richmond, BC) was used for the volume study and for implant guidance. The procedure workflow from the BC Cancer Agency was followed.

A couple of days before the implant, a set of transversal TRUS images of the phantom were acquired. A treatment plan was designed at the BC Cancer agency, and the plan was loaded into the robot controller described in the previous section. Note that the interface can load a text file from a Treatment Planning System (VariSeed, Varian Medical Systems, Charlottesville, VA) that contains the sequence of needle numbers and their coordinates. There were 26 needles with 136 seeds in the plan. The needles were loaded with dummy seeds. We used a combination of needles – some with loose seeds and some using stranded seeds (RAPIDStrand, Oncura, Plymouth Meeting, PA).

The robot-TRUS calibration was carried out by loading a needle, lowering it into a water tank, and resetting the robot origin according to the needle location in the TRUS transversal images.

The implant was carried out in the same manner as done in the operating room. The needle list was read out by a medical physics student, in the same way a brachytherapy technician would do in the operating room. The needles were inserted by a Radiation Oncologist, aiming for the same type of accuracy as normally done for a patient. The entire procedure was completed in 32 minutes, which compares favourably with the needle implant time of between 30 and 40 minutes at the BC Cancer Agency, especially since this was the first use of the setup (robot, ultrasound machine, and stepper) by the Radiation Oncologist.

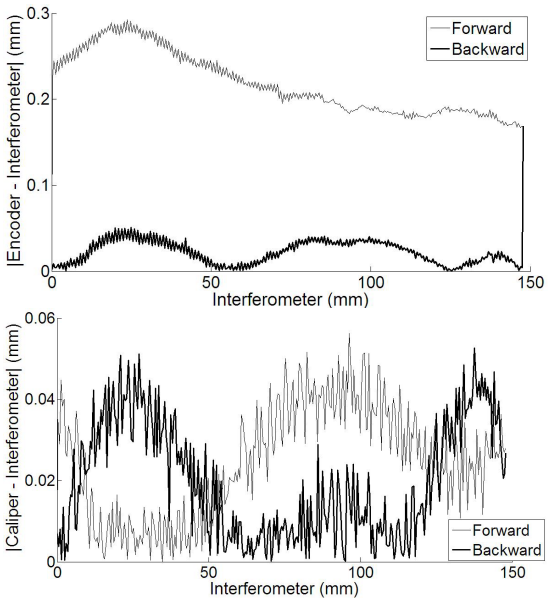

Fig. 6. X-axis displacement error and caliper reading error relative to interferometer reading.

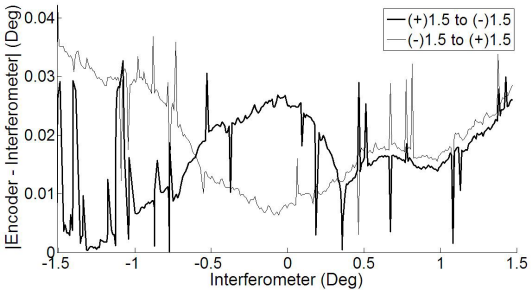

Fig. 7. Pitch angle θ_X error relative to interferometer reading.

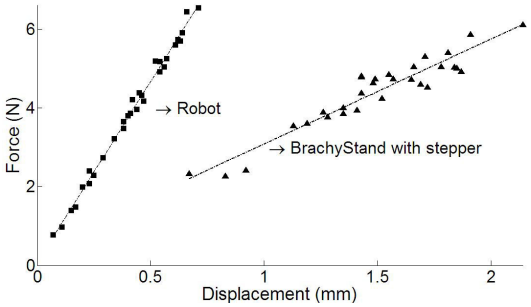

Fig. 8. *Y*-axis stiffness of the robot and CIVCO Brachyguide/EXII stabilizer/stepper stiffness.

We performed a post-implant CT scan (in-slice resolution 0.293mm/pixel, thickness 1.5mm) of the phantom. For each seed, we found the seed placement errors between the (*X,Y*) coordinates of the seeds in the CT scan and those of the pre-operative plan. Table II presents the error statistics. Fig. 10 presents the error histograms. Fig. 11 presents the projections of all the implanted seeds onto the plane orthogonal to the needle directions from the treatement plan. All needles in the implant were parallel to each other, as the treatment planning system currently available to us does not produce angled needles.

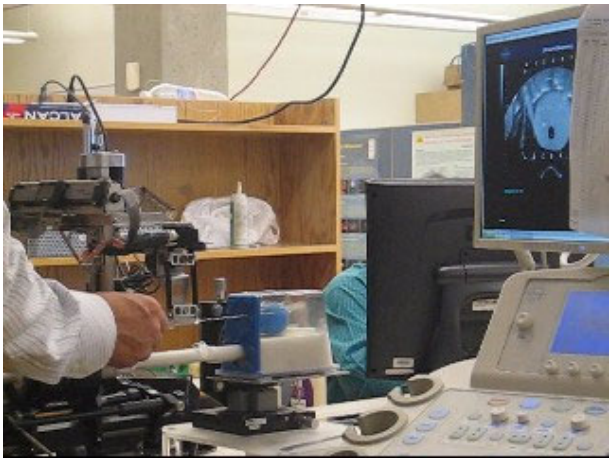

Fig. 9. Phantom implant performed in the laboratory.

The main goal of the experiment was to demonstrate that for prostate brachytherapy, the use of our robotic needle guide does not lead to increased procedure time.

V. Discussion

The Brachyguide design differs from other designs previously presented. One of its main advantages is the ability to manually position and orient the needle over its entire workspace when the power is off. Because the robot is not backdrivable, when the power is off, the needle guide stays put in position. No brakes are required, and, if necessary, the physician can operate the Brachyguide as a manual positioning stage with four degrees of freedom. Thus the implant plan can be carried out, even with angulated needle insertions, in case of electrical or software failure. This is not the case with previously reported designs. To deal with robot failure, the alternative and elegant approach from [10] allows the interchange of the robot with a targeting template, while other approaches require removing the TRUS, which is less desirable. Unless a special-purpose targeting grid is designed that allows for angulated needles, the interchange with a targeting template would require a change in the treatment plan, from one that has angulated needles to one that has parallel needles.

Because it is manually positioned, Brachyguide is not attached to the brachytherapy stepper by a quick release mechanism. It might be worthwhile to have such an attachment in the unlikely case of catastrophic mechanical failure, so that the robot could be detached immediately and replaced by a standard template or by a template modified to allow needle angulation.

In terms of design improvements, note that the Brachystand/EXII stepper combination is not stiff enough to carry the Brachyguide device without significant deflection. We are presently studying approaches to deal with this problem. Note however, that most of the flexing comes from the Brachystand stepper base and not from the flexing of the robot relative to the TRUS. The stiffness between the TRUS probe and the robot is much higher, and therefore implant accuracy relative to the TRUS is not affected.

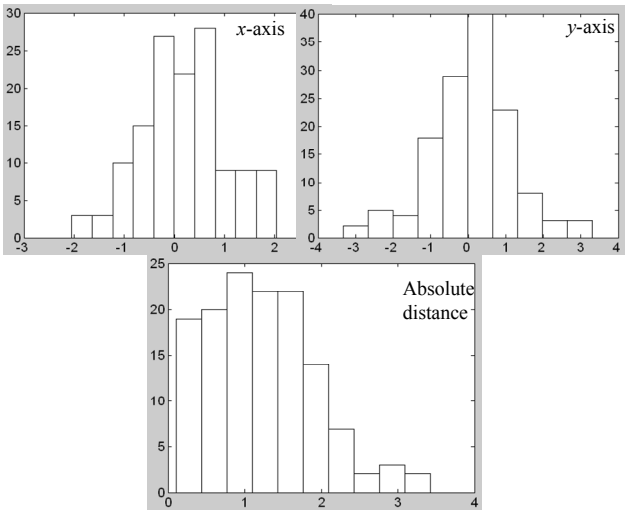

Fig. 10. Seed placement error histograms.

TABLE II: Statistics of Seed Placement Errors

	Maximum absolute error (mm)	Average error (mm)	Standard deviation of errors (mm)
Y-axis	3.3301	0.1080	1.1048
X-axis	2.0464	0.1993	0.8689
Distance in *XY* plane	3.4273	1.2296	0.7102

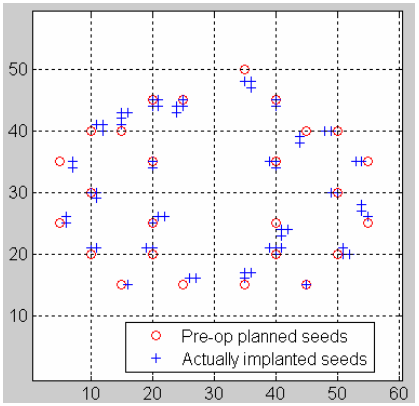

Fig. 11. Projection of the CT scan of the prostate phantom onto the plane orthogonal to the planned needle insertions.

The phantom implant that we carried out demonstrated very effective use of the robotic guide. We followed standard operating procedure and completed the implant in a very short time. While the reported time is for parallel needle insertions, very little of the procedure changes as a result of using angulated needles, so we expect to achieve similar completion times.

The implant accuracy, measured relative to the planned seed location, shows small errors, even though the results reported are affected by registration error (the TRUS was manually registered to the prostate phantom as done in the

operating room) and a relatively stiff CIRS tissue phantom that is not mechanically equivalent to the prostate region. Because the needle deflection and the phantom deformation are quite different from those occuring in human tissue, the phantom inplant data cannot really be correlated with future patient implants and simply serves to show the feasibility of our approach.

VI. Conclusion

We presented the design and characterization of a robotic guide for prostate brachytherapy. While other needle guides have been presented before for this and other applications, our design has a number of novel features. The device provides an un-encumbered view of the perineum, has minimum interference with the endorectal ultrasound probe, it can be used in manual mode, and uses an inherently safe design without brakes and with redundant sensing. Similarly, to the device presented in [10], this robotic needle guide can replace the guiding template attached to a conventional brachytherapy stepper.

The performance characterization of Brachyguide was completed based on measurements typically used for machine tools and demonstrates performance that is beyond that needed for brachytherapy. We will carry out minor design improvements in order to eliminate backlash and bring its performance close to the 0.06 mm translational repeatability enabled by the translational sensors. The rotational repeatability is already within the 0.05^{o} specified by the rotation stage manufacturer.

With the present interface, we have demonstrated that the use of the Brachyguide in a rather large phantom implant, achieved with good accuracy, does not increase the procedure time.

In future work, we are developing the planning algorithms that will make use of the capability of this device to deliver angled needles on a much finer grid than used in conventional procedures. We plan to integrate deformation models in such planning algorithms as described in [17], based on the patient-specific ultrasound elastography measurements described in [19].

A short video that demonstrates the operation of the Brachyguide robot accompanies this paper.

Acknowledgment

We would like to thank Dan Gelbart for his generous help with the design and building of the prototype. We thank Nick Chng and Xu Wen for their help with experiments, and Professors Yusuf Altintas and Xiaodong Lu for lending us the interferometer used in our measurements.

References

[1] A.L. Zietman. “Localized prostate cancer: brachytherapy.” *Curr. Treat. Options. Oncol.*, vol. 3, pp. 429-36, October 2002.

[2] M.R. Cooperberg, D.P. Lubeck , M.V. Meng, S.S. Mehta, and P.R. Carroll, “The Changing Face of Low-Risk Prostate Cancer: Trends in Clinical Presentation and Primary Management.” *Journal of Clinical Oncology*, vol. 22, pp. 2141-2149, June 2004.

[3] P. Wust , D.W. von Borczyskowski, T. Henkel, C. Rosner C, R. Graf, W. Tilly, V. Budach, R. Felix, and F. Kahmann, “Clinical and physical determinants for toxicity of 125-I seed prostate brachytherapy.” *Radiother. and Oncol.*, vol. 73, pp. 39-48, Oct 2004.

[4] M.J. Zelefsky, Y. Yamada, C. Marion, S. Sim, G. Cohen, L. Ben-Porat, D. Silvern, and M. Zaider, “Improved conformality and decreased toxicity with intraoperative computer-optimized transperineal ultrasound-guided prostate brachytherapy.” *Int. J. Radiat. Oncol. Biol. Phys.*, vol. 55, pp. 956-963, March 2003.

[5] A.G. Macdonald, M. Keyes, A. Kruk, G. Duncan, V. Moravan, and W.J. Morris, “Predictive factors for erectile dysfunction in men with prostate cancer after brachytherapy: Is dose to the penile bulb important?.” *International Journal of Radiation Oncology*Biology*Physics*, vol. 63, pp. 155-163, September 2005.

[6] F. Shao, K.V. Ling, W.S. Ng, and R.Y. Wu, “Prostate Boundary Detection From Ultrasonographic Images.” *J. US. in Med.*, vol. 22, pp. 605-623, June 2003.

[7] V. Lagerburg, M.A. Moerland,. J.J.W. Lagendijk, and J.J. Battermann, “Measurement of prostate rotation during insertion of needles for brachytherapy.” *Radiothera. Oncol.*, vol. 77, pp. 318 -323, Dec. 2005.

[8] S. Nag, J.P. Ciezki, R. Cormack, S. Doggett, K. DeWyngaert, G.K. Edmundson, R.G. Stock, N.N. Stone, Y. Yu, and M.J. Zelefsky, ”Intraoperative planning and evaluation of permanent prostate brachytherapy: Report of the American Brachytherapy Society.” *Int. J. Rad. Onc. Biol. Phys.*, vol. 51, pp. 1422-1430, December 2001.

[9] G. Fichtinger, E. C. Burdette, A. Tanacs, A. Patriciu, D. Mazilu, L.L. Whitcomb, and D. Stoianovici. "Robotically assisted prostate brachytherapy with transrectal ultrasound guidance – phantom experiments." *Brachytherapy*, vol. 5, pp. 14-26, January-March 2006.

[10] G. Fichtinger, J. Fiene, C.W. Kennedy, G. Kronreif, I. Iordachita, D.Y. Song, E. C. Burdette, and P. Kazanzides, “Robotic assistance for ultrasound guided prostate brachytherapy.” *Med. Image Comput. Comput. Assist. Interv*., vol. 10, pp. 119-27, 2007.

[11] Y. Yu, T. K. Podder, Y. Zhang, W-S. Ng, V. Misic, J. Sherman, L. Fu, D. Fuller, E. Messing, D.J. Rubens, J.G. Strang, and R. Brasacchio, “Robot-Assisted Prostate Brachytherapy.” *Med. Image Comput. Comput. Assist. Interv.*, vol. 9, pp. 41-49, 2006.

[12] Z. Wei, G. Wan, L. Gardi, G. Mills, D. Downey, A. Fenster, "Robot-assisted 3D-TRUS guided prostate brachytherapy: System integration and validation.” *Med. Phys.*, vol. 31, pp. 539-548, March 2004.

[13] J. Bax, L. Gardi, J. Montreuil, D. Smith, and A. Fenster, “A compact robotic apparatus and method for 3-D ultrasound guided prostate therapy.” *Proc. of SPIE*, Vol. 6509, pp. 2H1-8, March 2007.

[14] H. Bassan, T. Hayes, R.V. Patel, and M. Moallem, "A Novel Manipulator for 3D Ultrasound Guided Percutaneous Needle Insertion." *Proc. IEEE Intl. Conf. Rob. Aut.*, pp. 617-622, April 2007.

[15] S.P. DiMaio, G.S. Fischer, S.J. Maker, N. Hata, I. Iordachita, C.M. Tempany, R. Kikinis, and G. Fichtinger, “A System for MRI-guided Prostate Interventions.” *1st IEEE/RAS-EMBS Intl. Conference on Biomedical Robotics and Biomechatronics*, pp: 68- 73, 2006.

[16] R. Alterovitz, K. Goldberg, J. Pouliot, R. Taschereau, and I-Chow. Hsu, “Needle insertion and radioactive seed implantation in human tissues: simulation and sensitivity analysis.” *Proc. IEEE Int. Conf. Rob. Aut.*, vol. 2, pp. 1793–1799, September 2003.

[17] E. Dehghan and S. E. Salcudean, “Needle Insertion Point and Orientation Optimization in Non-linear Tissue with Application to Brachytherapy.” *IEEE Int. Conf. Rob. Aut.*, pp. 2267-72, April 2007.

[18] James T. Hing, Ari D. Brooks, and Jaydev P. Desai, “A Biplanar Fluoroscopic Approach for the Measurement, Modeling, and Simulation of Needle and Soft Tissue Interaction”, Medical Image Analysis, 11(1), pages 62-78, 2007.

[19] S.E. Salcudean, D. French, S. Bachmann, R. Zahiri-Azar, X. Wen, and W.J. Morris, “Viscoelasticity Modeling of the Prostate Region Using Vibro-elastography”, *Med. Image Comput. Comput. Assist. Interv*., vol. 9, pp. 389-96, 2006

[20] Kettenbach, J., Kronreif, G., Figl, M., et al.: “Robot-assisted biopsy using ultrasound guidance: initial results from in vitro tests.”, Eur. Radiol. 15, 765-771, 2005.